

# Properties of the $\Lambda(1405)$ Hyperon Measured at CLAS

Kei Moriya

with

Reinhard Schumacher

Carnegie Mellon University

September 15, 2009

# Outline

## 1 Introduction

- motivation for the study of the  $\Lambda(1405)$  – what is it?
- theory of the  $\Lambda(1405)$
- goals of this analysis

## 2 CLAS Analysis

- the g11a data set in CLAS at Jlab
- cuts to the data
- background
- fits to the lineshape

## 3 Results

- lineshape
- cross section
- spin-parity

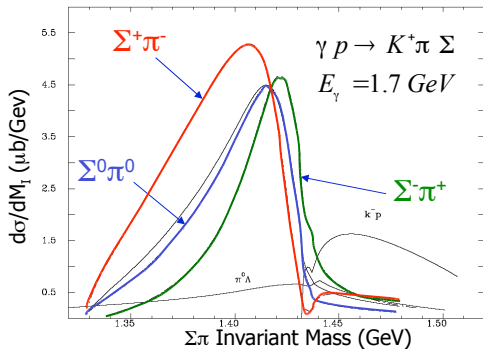
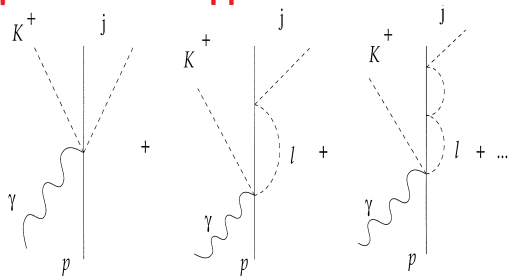
## 4 Conclusion

## what is the $\Lambda(1405)$ ?

- \*\*\*\* resonance just below  $N\bar{K}$  threshold
- $J^P = \frac{1}{2}^-$  (experimentally unconfirmed)
- can only be observed by reconstructing  $(\Sigma\pi)^0$  spectrum
- past experiments have found the lineshape (= invariant  $\Sigma\pi$  mass distribution) to be distorted from a simple Breit-Wigner form
- what is the nature of this distorted lineshape?
  - “normal”  $qqq$ -baryon resonance
  - $L = 1$  SU(3) singlet in constituent quark model
  - molecular  $N\bar{K}$  bound state
  - $uds$  singlet coupled to  $S$ -wave meson-baryon systems
  - $udsg$  hybrid,  $qqqq\bar{q}$
  - dynamically generated resonance in unitary coupled channel approach

# unitary coupled channel approach

dynamically generate  $\Lambda(1405)$



J. C. Nacher et al., Phys. Lett. B455, 55 (1999)

## difference in lineshape

$$\frac{d\sigma(\pi^+\Sigma^-)}{dM_I} \propto \frac{1}{2}|T^{(1)}|^2 + \frac{1}{3}|T^{(0)}|^2 + \frac{2}{\sqrt{6}}\text{Re}(T^{(0)}T^{(1)*}) + O(T^{(2)})$$

$$\frac{d\sigma(\pi^-\Sigma^+)}{dM_I} \propto \frac{1}{2}|T^{(1)}|^2 + \frac{1}{3}|T^{(0)}|^2 - \frac{2}{\sqrt{6}}\text{Re}(T^{(0)}T^{(1)*}) + O(T^{(2)})$$

$$\frac{d\sigma(\pi^0\Sigma^0)}{dM_I} \propto \frac{1}{3}|T^{(0)}|^2 + O(T^{(2)})$$

J. C. Nacher et al., Nucl. Phys. B455, 55

- difference in lineshapes is due to interference of isospin terms in calculation ( $T^{(I)}$  represents amplitude of isospin  $I$  term)

## goals of $\Lambda(1405)$ analysis

- measure the lineshape in the three  $\Sigma\pi$  channels ( $\Sigma^+\pi^-$ ,  $\Sigma^0\pi^0$ ,  $\Sigma^-\pi^+$ )
- measure the differential cross section (angular dependence)
- determine the spin and parity

**if distortion of lineshape is observed, this could be the first observation of a non- $qqq$  baryonic structure**

## the g11a data set taken at CLAS

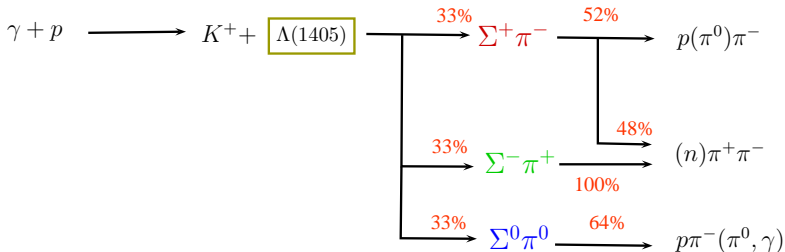
- ran from May to July 2004
- photoproduction experiment on a proton target
- photon energies from below  $\Lambda(1405)$  threshold to 3.84 GeV
- large dataset with  $\sim 20$  billion triggers
- current estimates of reconstructed  $\Lambda(1405)$  events:  $\sim 272\text{K}$

data is binned in:

- 10 bins of 100 MeV wide  $W$  bins
- $\sim 20$  bins of  $t$  in each  $W$  bin



## reaction of interest



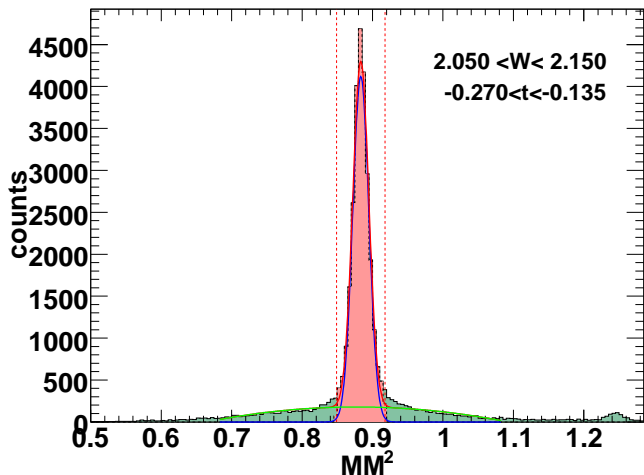
- 3  $\Sigma\pi$  decay channels (2 decay modes for  $\Sigma^+\pi^-$ )
- This will be the first experimental result to compare all 3  $\Sigma\pi$  decay modes



## decay channel selection cut

example in 1 bin:

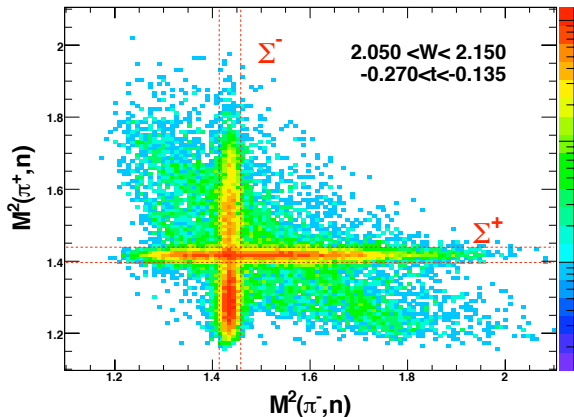
- $\gamma + p \rightarrow K^+ \pi^+ \pi^- (n)$
- detect  $K^+, \pi^+, \pi^-$ , reconstruct missing neutron
- fit to Gaussian and select  $\pm 3\sigma$  around neutron peak



## intermediate ground state hyperon

example in 1 bin:

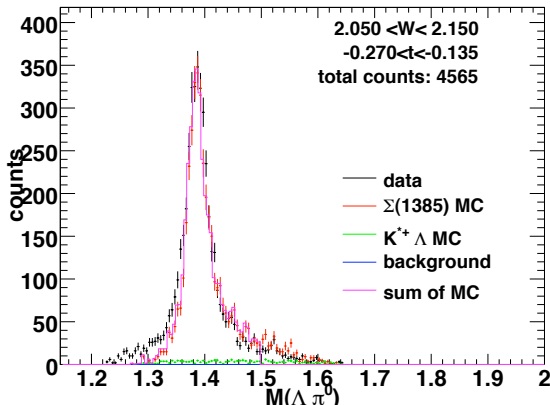
- neutron combined with  $\pi^\pm$  reconstructs  $\Sigma^\pm$
- project on each axis, select  $\pm 2\sigma$ , exclude other hyperon
- diagonal band ( $K^0$  from  $\pi^+\pi^-$ ) is also excluded



## background (1) – $\Sigma(1385)$

- close in mass and width to  $\Lambda(1405)$
- decays primarily to  $\Lambda\pi^0$  (B.R.  $\sim 88\%$ )
- small B.R. to  $\Sigma^\pm\pi^\mp$ :  $\sim 6\%$  each

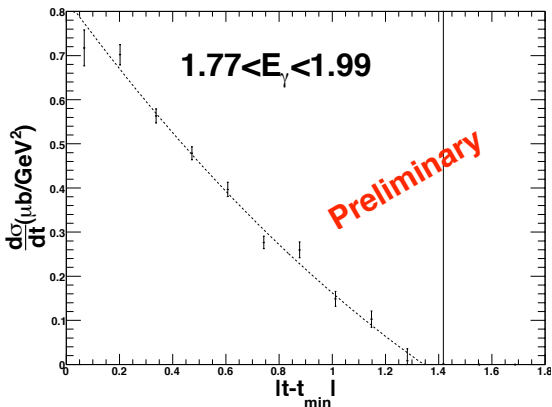
$\Rightarrow$  calculate  $\Sigma(1385)$  cross section in each bin from  $\Lambda\pi^0$  channel, then scale down by B.R. to extract yield in  $\Sigma\pi$  channels



## background (1) – $\Sigma(1385)$

- close in mass and width to  $\Lambda(1405)$
- decays primarily to  $\Lambda\pi^0$  (B.R.  $\sim 88\%$ )
- small B.R. to  $\Sigma^\pm\pi^\mp$ :  $\sim 6\%$  each

$\Rightarrow$  calculate  $\Sigma(1385)$  cross section in each bin from  $\Lambda\pi^0$  channel, then scale down by B.R. to extract yield in  $\Sigma\pi$  channels

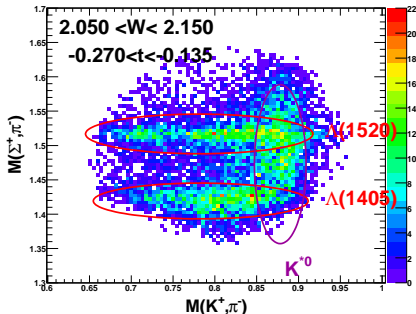


## background (2) – $K^{*0}\Sigma^+$

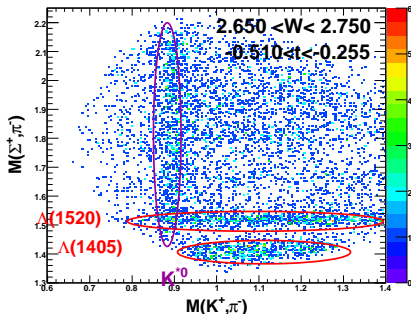
- $\Gamma \sim 50$  MeV
- strong overlap with  $\Lambda(1405)$  in lower  $W$  bins, separated at higher energies

⇒ generated MC and subtract off incoherently  
(checks need to be done for interference)

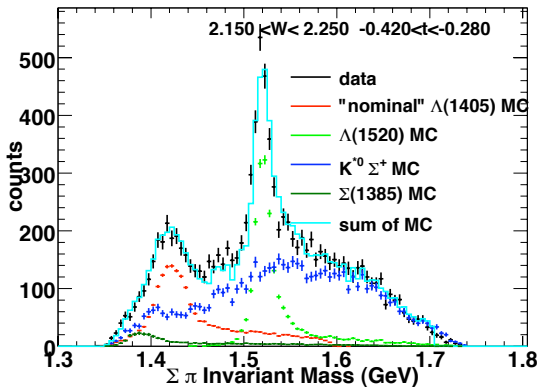
low energy bin



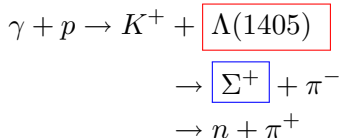
high energy bin



## example of fit to lineshape



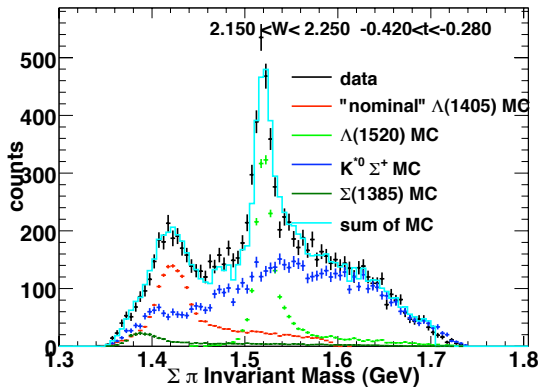
reaction:



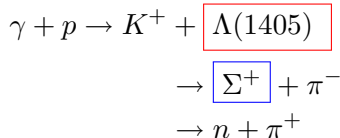
### "nominal" $\Lambda(1405)$

- Monte Carlo generated with PDG values of mass, width
- all Monte Carlo was processed through detector simulation
- after fitting, this process was iterated

## example of fit to lineshape



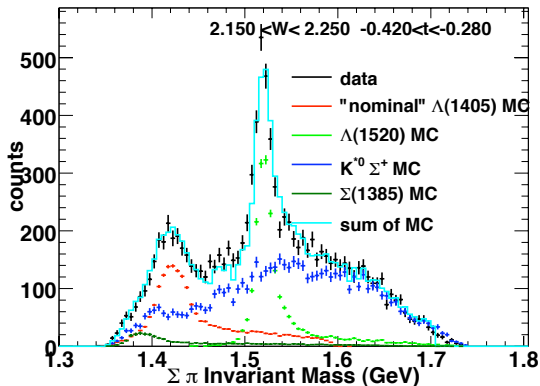
reaction:



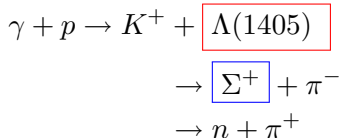
### $\Sigma(1385)$

- strong overlap with  $\Lambda(1405)$  due to close mass and width
- $\Lambda\pi^0$  decay mode was used to fix yield in  $\Sigma\pi$  decay modes
- Monte Carlo generated with PDG values of mass, width

## example of fit to lineshape



reaction:

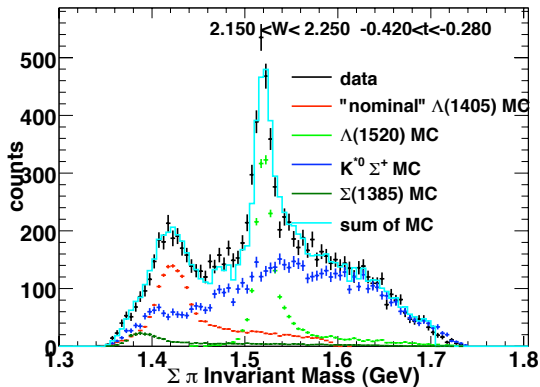


### $\Lambda(1520)$

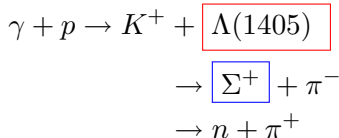
- Monte Carlo generated with PDG values of mass, width
- well-established Breit-Wigner lineshape



## example of fit to lineshape



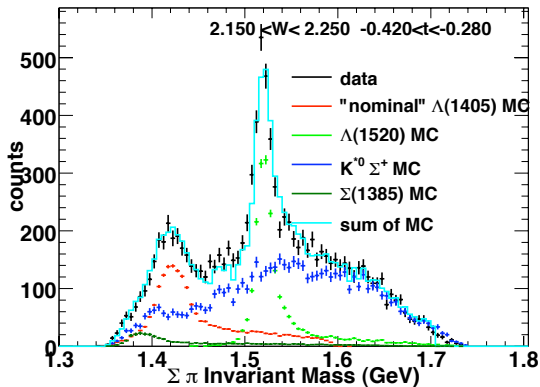
reaction:



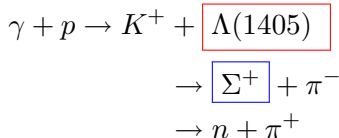
$K^{*0}$

- strong kinematic overlap with  $\Lambda(1405)$
- Monte Carlo generated with PDG values of mass, width

## example of fit to lineshape



reaction:

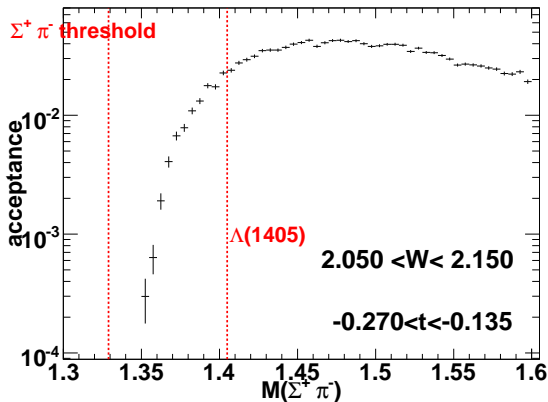


⇒ after fitting with the above templates, we subtracted off contributions from the  $\Sigma(1385)$ ,  $\Lambda(1520)$ ,  $K^{*0}$ , and assigned the remaining contribution to the  $\Lambda(1405)$

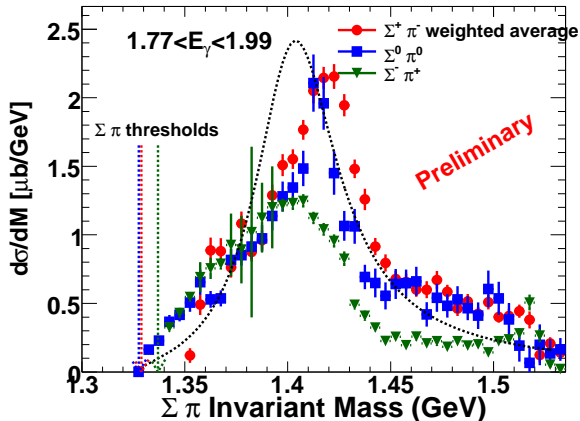
⇒ this process has been iterated

## acceptance correction

- after subtracting background contributions, we are left with “residual” spectrum
- to correct for dependence of the lineshape on acceptance, we have calculated the acceptance as a function of lineshape
- our lineshape results are summed over the  $t$  bins in each energy bin



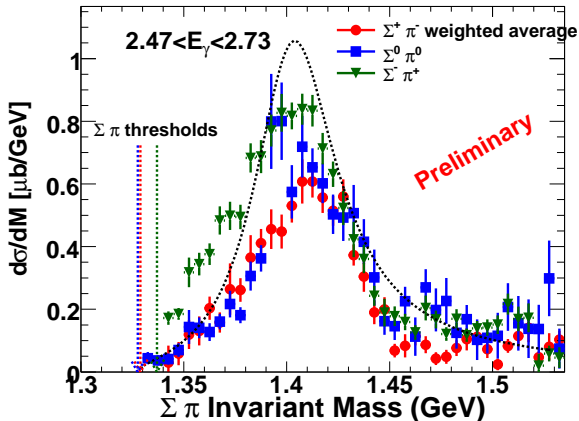
## results of lineshape after acceptance correction



different lineshapes for each  $\Sigma\pi$  decay mode

- lineshapes do appear different for each  $\Sigma\pi$  decay mode
- $\Sigma^+\pi^-$  decay mode has peak at highest mass, narrow than  $\Sigma^-\pi^+$

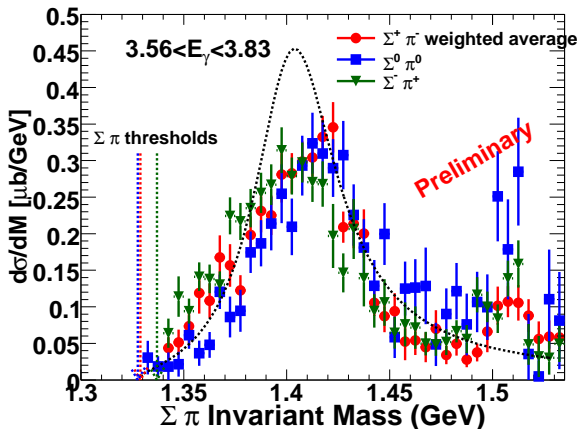
## results of lineshape after acceptance correction



different lineshapes for each  $\Sigma\pi$  decay mode

- lineshapes do appear different for each  $\Sigma\pi$  decay mode
- $\Sigma^+ \pi^-$  decay mode has peak at highest mass, narrow than  $\Sigma^- \pi^+$

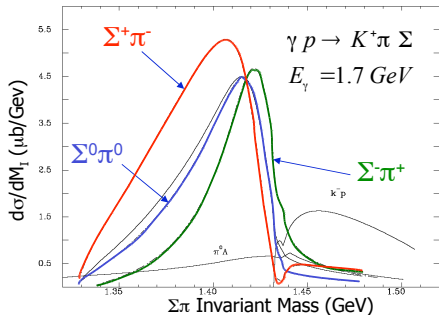
## results of lineshape after acceptance correction



different lineshapes for each  $\Sigma\pi$  decay mode

- lineshapes do appear different for each  $\Sigma\pi$  decay mode
- $\Sigma^+\pi^-$  decay mode has peak at highest mass, narrow than  $\Sigma^-\pi^+$

# theory prediction from chiral unitary approach



J. C. Nacher et al., Nucl. Phys. B455, 55

$$\begin{aligned} \frac{d\sigma(\pi^+\Sigma^-)}{dM_I} &\propto \frac{1}{2}|T^{(1)}|^2 + \frac{1}{3}|T^{(0)}|^2 + \frac{2}{\sqrt{6}}\text{Re}(T^{(0)}T^{(1)*}) + O(T^{(2)}) \\ \frac{d\sigma(\pi^-\Sigma^+)}{dM_I} &\propto \frac{1}{2}|T^{(1)}|^2 + \frac{1}{3}|T^{(0)}|^2 - \frac{2}{\sqrt{6}}\text{Re}(T^{(0)}T^{(1)*}) + O(T^{(2)}) \\ \frac{d\sigma(\pi^0\Sigma^0)}{dM_I} &\propto \frac{1}{3}|T^{(0)}|^2 + O(T^{(2)}) \end{aligned}$$

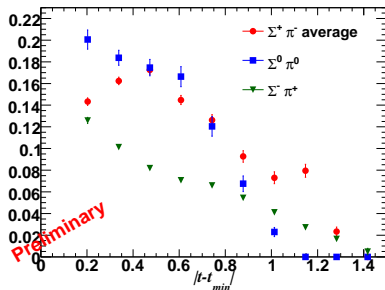
- $\Sigma^-\pi^+$  decay mode peaks at highest mass, most narrow
- difference in lineshapes is due to interference of isospin terms in calculation ( $T^{(I)}$  represents amplitude of isospin  $I$  term)

## differential cross sections

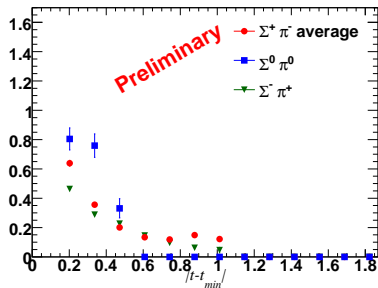
- summing over the lineshape gives differential cross section ( $M(\Sigma\pi) < 1.500$  GeV)
- $\Lambda(1520)$  serves as a check of systematics
- at lower energies where lineshapes differ, differences in  $\frac{d\sigma}{dt}$  are observed

$$\frac{d\sigma}{dt} [\mu\text{b}/\text{GeV}^2] \text{ for } 2.050 < W < 2.150 \text{ (GeV)}$$

$\Lambda(1405)$



$\Lambda(1520)$



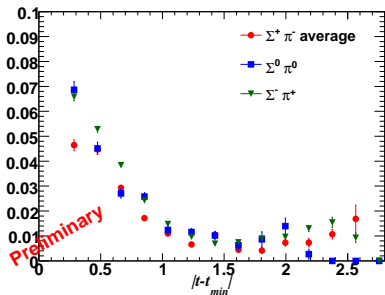


## differential cross sections

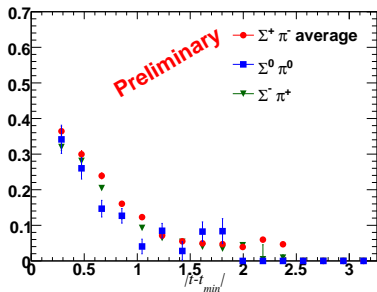
- summing over the lineshape gives differential cross section ( $M(\Sigma\pi) < 1.500$  GeV)
- $\Lambda(1520)$  serves as a check of systematics
- at lower energies where lineshapes differ, differences in  $\frac{d\sigma}{dt}$  are observed

$$\frac{d\sigma}{dt} [\mu\text{b}/\text{GeV}^2] \text{ for } 2.350 < W < 2.450 \text{ (GeV)}$$

$\Lambda(1405)$



$\Lambda(1520)$

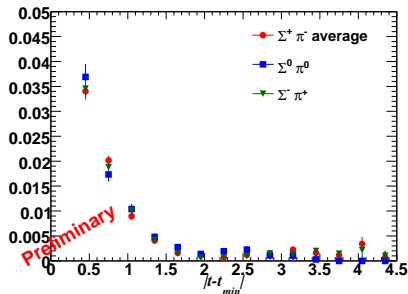


## differential cross sections

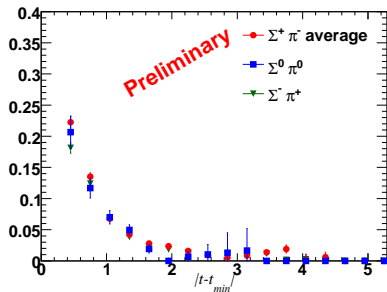
- summing over the lineshape gives differential cross section ( $M(\Sigma\pi) < 1.500$  GeV)
- $\Lambda(1520)$  serves as a check of systematics
- at lower energies where lineshapes differ, differences in  $\frac{d\sigma}{dt}$  are observed

$$\frac{d\sigma}{dt} [\mu\text{b}/\text{GeV}^2] \text{ for } 2.750 < W < 2.840 \text{ (GeV)}$$

$\Lambda(1405)$



$\Lambda(1520)$

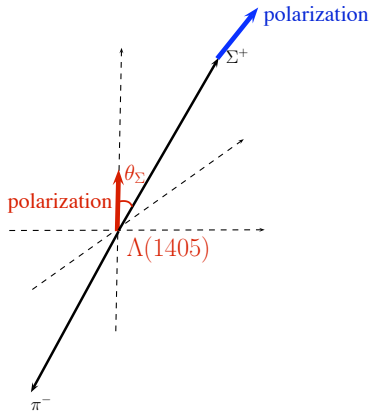


## $J^P$ of $\Lambda(1405)$

no previous **direct experimental evidence** for the spin and parity  
(PDG assumes  $1/2^-$ ) "Note on the  $\Lambda(1405)$ " 2000 PDG, R.H. Dalitz

How do we measure these quantities?

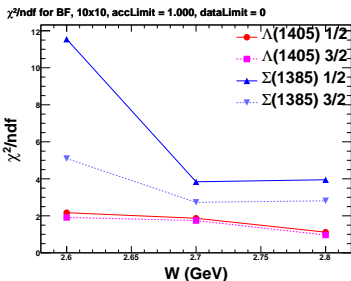
- **spin** – measure distribution into  $\Sigma\pi$ 
  - flat distribution is best evidence possible for  $J = 1/2$
- **parity** – measure polarization of  $\Sigma$  from  $\Lambda(1405)$ 
  - Polarization direction as a function of  $\Sigma$  decay angle will be determined by  $J^P$  of  $\Lambda(1405)$



## determination of spin

fits to  $J = \frac{1}{2}, \frac{3}{2}$  distributions done to  
 $\Lambda(1405) \rightarrow \Sigma^+ \pi^- / \Sigma(1385) \rightarrow \Lambda \pi^0$

- 3 bins of  $W$  centered at 2.6, 2.7, 2.8 GeV with forward  $K^+$  angles
- selected region has kinematic separation from  $K^{*0}$  background



distribution of  $J = 1/2$ :

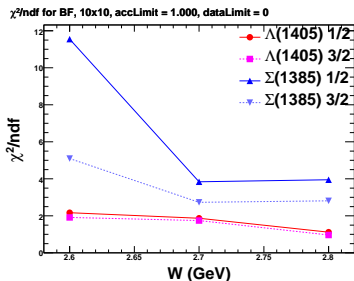
$$I(\theta, \phi) = \frac{C}{4\pi}$$

(no parameters for shape of distribution)

## determination of spin

fits to  $J = \frac{1}{2}, \frac{3}{2}$  distributions done to  
 $\Lambda(1405) \rightarrow \Sigma^+ \pi^- / \Sigma(1385) \rightarrow \Lambda \pi^0$

- 3 bins of  $W$  centered at 2.6, 2.7, 2.8 GeV with forward  $K^+$  angles
- selected region has kinematic separation from  $K^{*0}$  background



distribution of  $J = 3/2$  ( $z$ -axis in production plane):

$$I(\theta, \phi) = \frac{C}{4\pi} \left[ 1 - \sqrt{5}t_2^0 \left( \frac{3}{2} \cos^2 \theta - \frac{1}{2} \right) + \Re t_2^1 \sqrt{\frac{15}{2}} \sin 2\theta \cos \phi - \Re t_2^2 \sqrt{\frac{15}{2}} \sin^2 \theta \cos 2\phi \right]$$

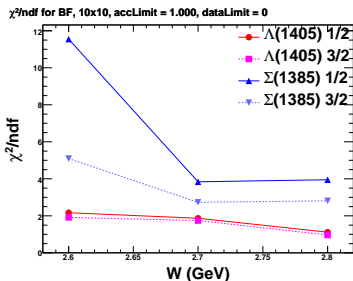
(3 parameters for shape of distribution)

( $t_L^M$  are “multipole parameters” N. Byers CERN report 67-20)

## determination of spin

fits to  $J = \frac{1}{2}, \frac{3}{2}$  distributions done to  
 $\Lambda(1405) \rightarrow \Sigma^+ \pi^- / \Sigma(1385) \rightarrow \Lambda \pi^0$

- 3 bins of  $W$  centered at 2.6, 2.7, 2.8 GeV with forward  $K^+$  angles
- selected region has kinematic separation from  $K^{*0}$  background



distribution of  $J = 3/2$  ( $z$ -axis out of production plane):

$$I(\theta, \phi) = \frac{C}{4\pi} \left[ 1 - \sqrt{5}t_2^0 \left( \frac{3}{2} \cos^2 \theta - \frac{1}{2} \right) - \Re t_2^2 \sqrt{\frac{15}{2}} \sin^2 \theta \cos 2\phi - \Im t_2^2 \sqrt{\frac{15}{2}} \sin^2 \theta \sin 2\phi \right]$$

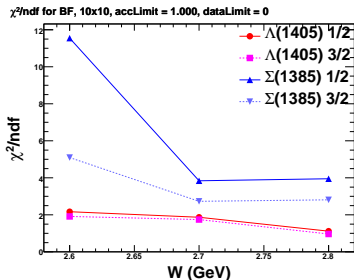
(3 parameters for shape of distribution)

( $t_L^M$  are “multipole parameters” N. Byers CERN report 67-20)

## determination of spin

fits to  $J = \frac{1}{2}, \frac{3}{2}$  distributions done to  
 $\Lambda(1405) \rightarrow \Sigma^+ \pi^- / \Sigma(1385) \rightarrow \Lambda \pi^0$

- 3 bins of  $W$  centered at 2.6, 2.7, 2.8 GeV with forward  $K^+$  angles
- selected region has kinematic separation from  $K^{*0}$  background

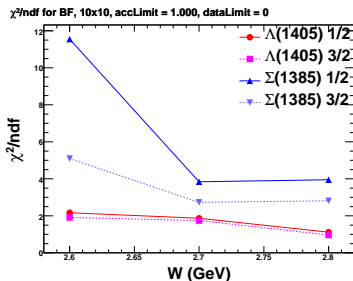


with  $J = 3/2$  fit,  $\chi^2/\text{ndf}$  is reduced for  $\Sigma(1385)$ ,  
but almost no reduction for  $\Lambda(1405)$

## determination of spin

fits to  $J = \frac{1}{2}, \frac{3}{2}$  distributions done to  
 $\Lambda(1405) \rightarrow \Sigma^+ \pi^- / \Sigma(1385) \rightarrow \Lambda \pi^0$

- 3 bins of  $W$  centered at 2.6, 2.7, 2.8 GeV with forward  $K^+$  angles
- selected region has kinematic separation from  $K^{*0}$  background



with  $J = 3/2$  fit,  $\chi^2/\text{ndf}$  is reduced for  $\Sigma(1385)$ ,  
but almost no reduction for  $\Lambda(1405)$

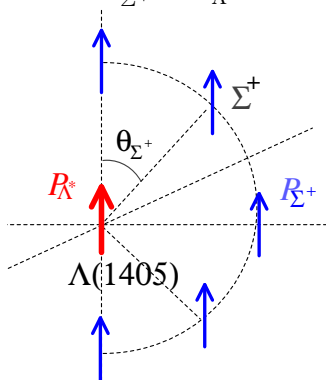
⇒ best possible evidence for  $J = 1/2$



## s-wave, p-wave scenario

$L = 0$  (s-wave)

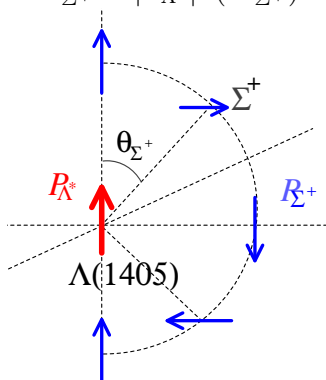
$$\vec{P}_{\Sigma^+} = \vec{P}_{\Lambda^*}$$



$\Lambda(1405) \rightarrow \Sigma\pi$  is *s*-wave  
 $\Leftrightarrow J^P = 1/2^-$

$L = 1$  (p-wave)

$$\vec{P}_{\Sigma^+} = |\vec{P}_{\Lambda^*}| \hat{n}(2\theta_{\Sigma^+})$$

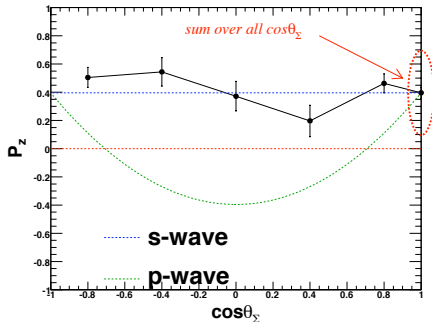


$\Lambda(1405) \rightarrow \Sigma\pi$  is *p*-wave  
 $\Leftrightarrow J^P = 1/2^+$

## determination of parity

polarization of  $\Lambda(1405)$  in direction  $\perp$  to production plane is measured

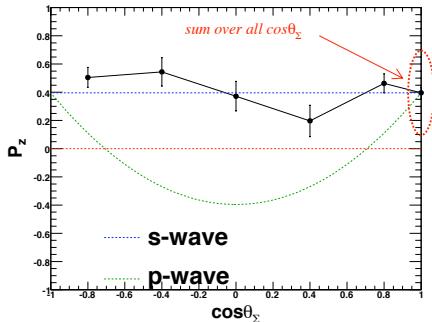
- $W = 2.6$  GeV
- forward  $K^+$  angles
- use reaction:  
 $\Lambda(1405) \rightarrow \Sigma^+ \pi^-$ ,  
 $\Sigma^+ \rightarrow p \pi^0$
- very large hyperon decay parameter  $\alpha = -0.98$



## determination of parity

polarization of  $\Lambda(1405)$  in direction  $\perp$  to production plane is measured

- $W = 2.6$  GeV
- forward  $K^+$  angles
- use reaction:  
 $\Lambda(1405) \rightarrow \Sigma^+ \pi^-$ ,  
 $\Sigma^+ \rightarrow p \pi^0$
- very large hyperon decay parameter  $\alpha = -0.98$

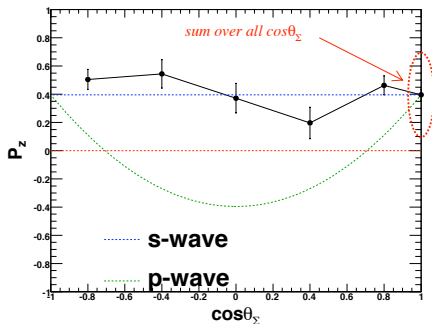


polarization does not change with  $\Sigma^+$  angle ( $\theta_{\Sigma^+}$ )

## determination of parity

polarization of  $\Lambda(1405)$  in direction  $\perp$  to production plane is measured

- $W = 2.6$  GeV
- forward  $K^+$  angles
- use reaction:  
 $\Lambda(1405) \rightarrow \Sigma^+ \pi^-$ ,  
 $\Sigma^+ \rightarrow p \pi^0$
- very large hyperon decay parameter  $\alpha = -0.98$



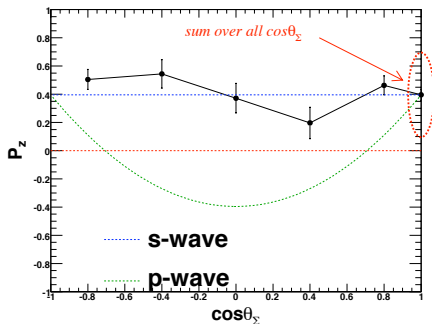
polarization does not change with  $\Sigma^+$  angle ( $\theta_{\Sigma^+}$ )

$\Rightarrow J^P = 1/2^-$  is confirmed

## determination of parity

polarization of  $\Lambda(1405)$  in direction  $\perp$  to production plane is measured

- $W = 2.6$  GeV
- forward  $K^+$  angles
- use reaction:  
 $\Lambda(1405) \rightarrow \Sigma^+ \pi^-$ ,  
 $\Sigma^+ \rightarrow p \pi^0$
- very large hyperon decay parameter  $\alpha = -0.98$



polarization does not change with  $\Sigma^+$  angle ( $\theta_{\Sigma^+}$ )

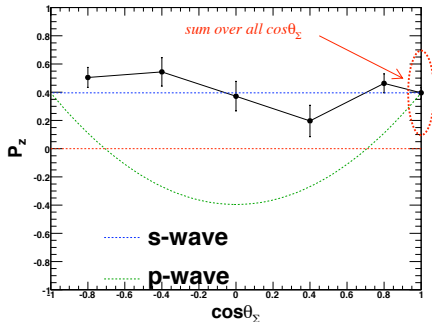
$\Rightarrow J^P = 1/2^-$  is confirmed

furthermore, this measured  $\Sigma^+$  polarization is the  $\Lambda(1405)$  polarization

## determination of parity

polarization of  $\Lambda(1405)$  in direction  $\perp$  to production plane is measured

- $W = 2.6$  GeV
- forward  $K^+$  angles
- use reaction:  
 $\Lambda(1405) \rightarrow \Sigma^+ \pi^-$ ,  
 $\Sigma^+ \rightarrow p \pi^0$
- very large hyperon decay parameter  $\alpha = -0.98$



polarization does not change with  $\Sigma^+$  angle ( $\theta_{\Sigma^+}$ )

$\Rightarrow J^P = 1/2^-$  is confirmed

furthermore, this measured  $\Sigma^+$  polarization is the  $\Lambda(1405)$  polarization

$\Rightarrow \Lambda(1405)$  is produced with  $\sim +40\%$  polarization

## conclusion

- high statistics measurement of  $\Lambda(1405)$  photoproduction has been done with CLAS at Jlab
- **difference in lineshape** has been observed
- **difference in differential cross section** has been observed
- **spin and parity are experimentally established for the first time**
- **polarization of  $\Lambda(1405)$  is found to be  $\sim +40\%$  at  $W \sim 2.6$  GeV, forward  $K^+$  angles**

⇒ **best evidence to date of possible deviation from a simple *qqq*-structure.**